Eur. Phys. J. D **43**, 173–176 (2007)
DOI: 10.1140/epjd/e2007-00078-8

THE EUROPEAN PHYSICAL JOURNAL D

A new real-space algorithm for realistic density functional calculations

E. Krotscheck[1,a], E.R. Hernández[2], S. Janecek[1], M.S. Kaczmarski[2,3], and R. Wahl[1]

[1] Institut für Theoretische Physik, Johannes Kepler Universität, Altenbergerstr. 69, 4040 Linz, Austria
[2] Institut de Ciència de Materials de Barcelona (ICMAB–CSIC) Campus de Bellaterra, 08193 Barcelona, Spain
[3] Institute of Physics, University of Silesia, Uniwersytecka 4, 40-007 Katowice, Poland

Received 23 July 2006 / Received in final form 17 October 2006
Published online 24 May 2007 –

Abstract. We present the implementation of a fast real-space algorithm for density functional calculations for atomic nanoclusters. The numerical method is based on a fourth-order operator splitting technique for the solution of the Kohn-Sham equation [1]. The convergence of the procedure is about one order of magnitude better than that of previously used second-order operator factorizations. The method has now been extended to deal with non-local pseudopotentials of the Kleinman-Bylander [2] type, permitting calculations for realistic systems, without significantly degrading the convergence rate. We demonstrate the convergence of the method for the examples C and C_{60} and present examples of structure calculations of Na and Mg clusters.

PACS. 71.15.Mb Density functional theory, local density approximation, gradient and other corrections – 61.46.Bc Clusters

1 Introduction: operator factorization

Real space methods where the Kohn-Sham wave functions, densities, and potentials are represented on a grid in coordinate space are rapidly gaining popularity [3]. Key to the applicability of the method is a fast and accurate solver for the Kohn-Sham equation. A powerful strategy is to apply the diffusion operator $\mathcal{T}(\epsilon) = e^{-\epsilon H}$ on a set of trial wave functions $\{\psi_i\}, i = 1 \ldots n$. After each step, the wave functions are orthonormalized; the process then converges towards the n lowest eigenfunctions of the Hamiltonian.

The diffusion operator $\mathcal{T}(\epsilon)$ can not be calculated exactly; we have recently [4] demonstrated that fourth order factorizations [5,6] of the diffusion operator $\mathcal{T}(\epsilon) = e^{-\epsilon H}$ can be used very effectively for local Hamiltonians $H_{\rm loc} = T + V$. One possible factorization is

$$\mathcal{T}^{(4)}(\epsilon) = e^{-\frac{\epsilon}{6}V} e^{-\frac{\epsilon}{2}T} e^{-\frac{2\epsilon}{3}\tilde{V}} e^{-\frac{\epsilon}{2}T} e^{-\frac{\epsilon}{6}V} = \mathcal{T}(\epsilon) + \mathcal{O}(\epsilon^5) \tag{1}$$

where

$$\tilde{V} = V + \frac{\epsilon^2}{48}[V,[T,V]] = V + \frac{\epsilon^2\hbar^2}{48m}|\nabla V|^2 \tag{2}$$

is an auxiliary, positive, local potential.

Local Hamiltonians are unfortunately insufficient for a quantitative description of many realistic systems; for example, the interaction of the valence electrons with the ion cores depends on energy and angular momentum. Thus, the Hamiltonian will normally have the form

$$H = T + V_{\rm loc} + V_{\rm nl}. \tag{3}$$

Using the Kleinman-Bylander [2] separable form of the ionic pseudopotentials, the non-local part of the Hamiltonian reads

$$\begin{aligned} V_{\rm nl}(\mathbf{r},\mathbf{r}') &= \sum_{i=1}^{N} v_{\rm nl}^{(i)}(\mathbf{r}-\mathbf{R}_i, \mathbf{r}'-\mathbf{R}_i) \\ &= \sum_{i=1}^{N}\sum_{\ell m} A_\ell^{(i)} \left\langle \mathbf{r}-\mathbf{R}_i \middle| P_{\ell m}^{(i)} \right\rangle \left\langle P_{\ell m}^{(i)} \middle| \mathbf{r}'-\mathbf{R}_i \right\rangle . \end{aligned} \tag{4}$$

In the above equation, $A_\ell^{(i)}$ are numerical constants characterizing the pseudopotential, and the $P_{\ell m}^{(i)}$ are projectors defined as $P_{\ell m}^{(i)} = R_\ell^{(i)}(r) Y_{\ell m}$, where $R_\ell(r)$ is a radial function, and $Y_{\ell m}$ are spherical harmonics; the $\mathbf{R}_i$ are the positions of the ions, and the superscript *(i)* indicates that the $A_\ell^{(i)}$, $P_{\ell m}^{(i)}$ and $R_\ell^{(i)}$ depend on the chemical species of atom i. The range of the non-local pseudopotential extends only up to a distance $r_c^{(i)}$ from each atomic position $\mathbf{R}_i$. Normally the core radii $r_c^{(i)}$ are chosen such that there is no overlap between the different core spheres.

To implement non-local potentials, the factorization is best carried out recursively. The computationally most

[a] e-mail: eckhard.krotscheck@jku.at

efficient form is

$$e^{-\epsilon H} = e^{-\frac{\epsilon}{6}V_{\rm nl}} e^{-\frac{\epsilon}{2}H_{\rm loc}} e^{-\frac{2\epsilon}{3}\tilde{V}_{\rm nl}} e^{-\frac{\epsilon}{2}H_{\rm loc}} e^{-\frac{\epsilon}{6}V_{\rm nl}} + \mathcal{O}(\epsilon^5)\,, \quad (5)$$

where $H_{\rm loc} = T + V_{\rm loc}$, and $\tilde{V}_{\rm nl}$ is defined analogously to equation (2),

$$\tilde{V}_{\rm nl} = V_{\rm nl} + \frac{\epsilon^2}{48}\left[V_{\rm nl}, [H_{\rm loc}, V_{\rm nl}]\right]\,. \quad (6)$$

The factors containing $H_{\rm loc}$ in the exponent are in turn factorized in terms of T and $V_{\rm loc}$ as indicated by equation (1). The double commutator $[V_{\rm nl}, [H_{\rm loc}, V_{\rm nl}]]$ has a projector structure similar to the pseudopotential itself; its exponential can therefore also be evaluated easily and exactly.

Since the factorized form of the diffusion operator is not exact, the eigenvalue/eigenfunction pairs acquire a dependence on the imaginary time step ϵ, their exact value being obtained in the limit $\epsilon \to 0$. On the other hand, the larger ϵ is, the faster the convergence will be. It is therefore desirable to have an approximation of the diffusion operator that is accurate for large values of ϵ. This is exactly where the fourth order factorizations are useful.

2 Numerical tests

The purpose of this section is to demonstrate the functionality of the fourth order factorization for real-space electronic structure calculations involving non-local pseudopotentials. We have chosen four different cases, namely, an isolated carbon atom, the diatomic molecule CO, the medium-size C_6H_6 benzene molecule, and the relatively large C_{60} cluster. These different cases allow us to probe different aspects of the method, as discussed below. Tests of the efficiency of the second and fourth order eigensolvers have been performed as follows: we have first solved the Kohn-Sham equations, taking the Perdew-Wang density functional [7] and employing Troullier-Martins [8] pseudopotentials generated by the program FHI98PP [9]. We have used projector functions for the $\ell = 0, 1, 2$ angular momentum channels, where the $\ell = 2$ projector was taken as the local potential. The cutoff radii have been $1.37a_0$ for the oxygen ion, and $1.46a_0$ for carbon. The orthogonalization and the density update were performed as described in reference [4]. We have then taken the electron density and the corresponding Kohn-Sham potential as a fixed local field and have solved again the eigenvalue problem, taking as initial guess for the evolution the wave functions of a particle in a box, and repeating the process for a sequence of time steps ϵ.

Figures 1 and 2 show the convergence of the lowest eigenvalue of a single C atom and a C_{60} cluster as a function of the time step for both a second order and a fourth order calculation. The isolated C atom is spherically symmetric, we can observe precise second or fourth order convergence over two and a half orders of magnitude of the time step, down to relative accuracies of 10^{-7}. It is useful to note that the ultimate accuracy of eigenvalues $e_i(\epsilon)$ is approximately given by the total evolved time $\tau = N\epsilon$, where N is the number of iterations. The necessary evolution time τ to reach a certain accuracy is characteristic of the system, but depends only weakly on the particular algorithm used and on the value of ϵ. Therefore, the horizontal distance between the two curves at a given error yields a direct estimate for the relative number of iterations between a second order and a fourth order factorization needed to obtain a given accuracy and, hence, the speed advantage of the fourth order over the second order method.

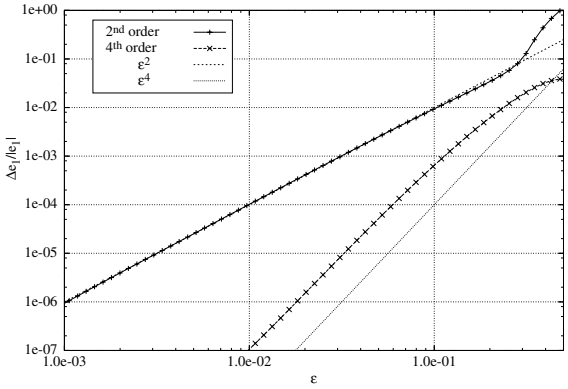

Fig. 1. The figure shows the relative error of the lowest eigenvalue of electrons in a single C atom on a double-logarithmic scale for the second and the fourth order algorithm. Also shown are the functions ϵ^2 and ϵ^4 to verify the power-law convergence. A cubic grid of 48^3 mesh points has been used for the calculation, with a resolution of $h = 0.3a_0$.

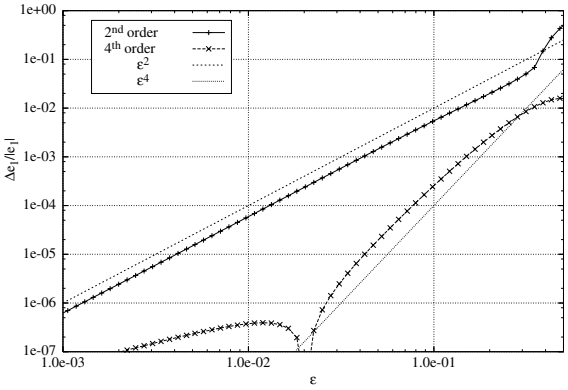

Fig. 2. Same as Figure 1 for a C_{60} molecule. A cubic grid of 64^3 mesh points has been used for the calculation, with a resolution of $h = 0.4a_0$.

For the C_{60} cluster we see a deviation from the fourth order convergence at accuracies better than 10^{-6}. This comes from an approximate evaluation of the double commutator term $[V_{\rm nl}\,[H_{\rm loc}, V_{\rm nl}]]$ where we have assumed, for simplicity, that the local potential in the vicinity of the individual carbon atoms is spherically symmetric. This approximation simplifies the numerical treatment enormously; it does not affect the final result and, as seen in Figure 2, affects the convergence only when a very good absolute accuracy has already been reached. We conclude this section by noting that the convergence features of

Table 1. CO equilibrium distances d_0 and harmonic vibrational frequencies ν obtained from a quadratic fit to the CO binding energy in the range [2.06 : 2.20]. h is the grid resolution in units of the Bohr radius, and N is the number of grid points in each direction. The entry labeled with ABINIT was obtained with the ABINIT code [10].

	d_0 $[a_0]$	ν [cm^{-1}]
$h = 0.2$ $N = 64$, unfiltered	2.12185	2117
$h = 0.2$ $N = 64$, filtered	2.12180	2119
$h = 0.4$ $N = 48$, unfiltered	2.10555	2299
$h = 0.4$ $N = 48$, filtered	2.10726	2153
$h = 0.6$ $N = 32$, filtered	2.13422	2036
ABINIT	2.113	2149

other molecules and higher lying states are basically the same.

To assess the numerical accuracy of our code, we have calculated the bond length and the vibrational frequency of a CO molecule as a function of discretization and grid size and compared these results with results from the ABINIT code [10]. Table 1 collects the equilibrium distances d_0 and harmonic vibrational frequencies ν for the CO molecule for different discretizations. To retain numerical accuracy even for rather coarse grids, we used a filtering method of Ono and Hirose [11]. The equilibrium distances for all acceptable calculations agree within better than 0.5 percent. The uncertainty of the vibrational frequency is somewhat larger, the $h = 0.6a_0$ result is 4 percent below the best value whereas the filtered $h = 0.4a_0$ result is 2 percent below the best value. We conclude that even a rather coarse mesh can lead, when used with sufficient care, to very good results — note that the calculation for the $h = 0.6a_0$ resolution is about thirty times faster than the best calculation. A more detailled description of the method and its convergence rate will be given elsewhere [12].

3 Applications: Na and Mg clusters

We have performed extensive calculations on the energetics and structure of neutral and charged Na and Mg clusters of up to 10 atoms, using pseudopotentials constructed by Fiolhas et al. [13] and Kümmel et al. [14]. Equilibrium configurations were found, starting from random configurations, by simulated annealing utilizing first Langevin and close to the equilibrium configuration damped Verlet moves. The calculations were repeated several times to find isomers. As an example we show the equilibrium structure of a Na_5 and a Mg_9 cluster in Figures 3 and 4.

Our calculated bond lengths differ from the theoretical values of Moullet et al. [15], Solov'yov et al. [16] and Lyalin et al. [17] by less then 10 percent. This discrepancy is most likely due to the use of local pseudopotentials for Na and Mg. While previous calculations were either all-electron [16,17] or else employed non-local pseudopotentials [15], in this work our aim has been to illustrate the methodology, rather than to obtain accurate values.

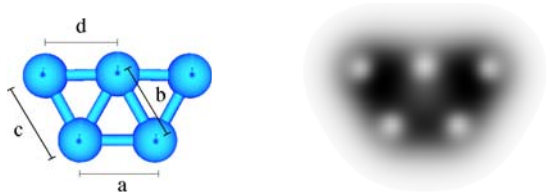

Na_5	a $[a_0]$	b $[a_0]$	c $[a_0]$	d $[a_0]$
Moullet et al. [15]	6.6	6.4	6.4	6.4
Solov'yov et al. [16]	6.80	6.66	6.73	6.69
this work using [14]	6.587	6.786	6.473	6.389
this work using [13]	6.640	6.805	6.511	6.437

Fig. 3. The figure shows the ion configuration (left panel) and the electron density (right panel, darker areas correspond to higher densities) of the equilibrium configuration of a Na_5 cluster. The attached table gives, for comparison, the theoretical bond lengths of Moullet et al. [15] and of Solov'yov et al. [16].

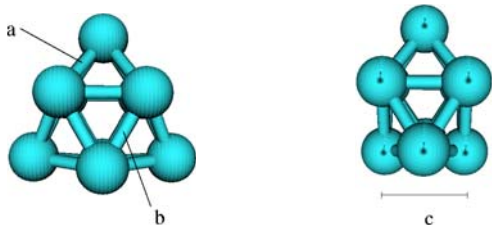

Mg_9	a $[a_0]$	b $[a_0]$	c $[a_0]$
Lyalin et al. [17]	5.792	6.039	5.938
this work	6.308	6.451	6.451

Fig. 4. The figure shows two views of the ground state configuration of a Mg_9 cluster. The table gives a comparison of our bond lengths with the calculations of Lyalin et al. [17].

We have also calculated energetic properties like ionization and dissociation energies. The ionization energies are defined as

$$V_n^{\rm ion} = E_n^+ - E_n. \tag{7}$$

Figures 5 and 6 demonstrate the reasonable agreement of our calculations with experimental data compiled by de Heer [18], and with theoretical calculations including all-electron calculations by Solov'yov et al. [16] (for Na), as well as calculations by Lyalin et al. [17], Akola et al. [19], and Reuse et al. [20] (for Mg). Furthermore we see in Figure 5 that a significant decrease happens at the transition of Na_2 to Na_3 and of Na_8 to Na_9. This is due to the closure of the $1s$ and $1p$ shell of the delocalized electrons in Na_2 and Na_8.

The dissociation energy for the decomposition of a cluster of size n for the mth dissociation channel, $Na_n^{(+)} \to Na_{n-m}^{(+)} + Na_m$, is given by

$$E_m^{\rm diss}(Na_n^{(+)}) = E(Na_n^{(+)}) - \Big[E(Na_{n-m}^{(+)}) + E(Na_m)\Big]. \tag{8}$$

Figure 7 indicates that most clusters decay by expulsion of a single Na atom, Only Na_5 and Na_7 deviate, they dissociate under the formation of a sodium dimer. Our results for

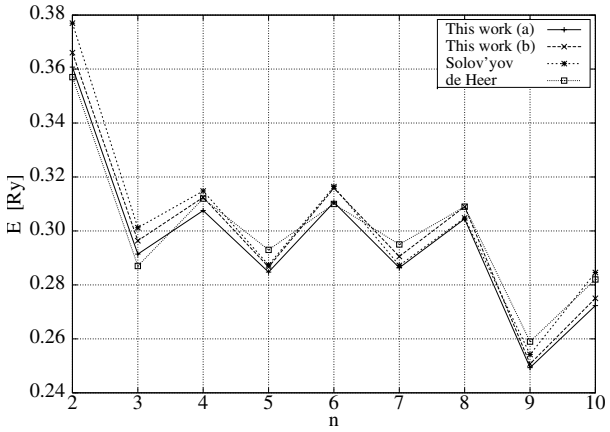

Fig. 5. Ionization energies for Na_n clusters. Curve labels (a) and (b) are our calculations, using the pseudopotentials of references [13,14], respectively. The short-dashed line marked with stars is from the calculations by Solov'yov [16], and the dotted line marked with boxes from the compilation of experimental data by de Heer [18].

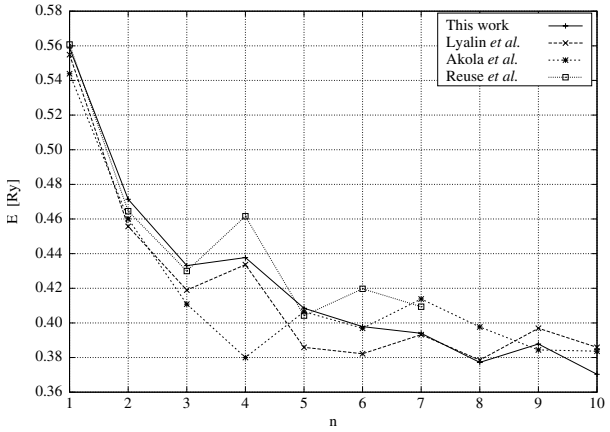

Fig. 6. Ionization energies for Mg_n clusters. This work has been based on the local pseudopotentials of reference [13], also shown are calculations by Lyalin et al. [17], Akola et al. [19], and Reuse et al. [20] as marked in the figure.

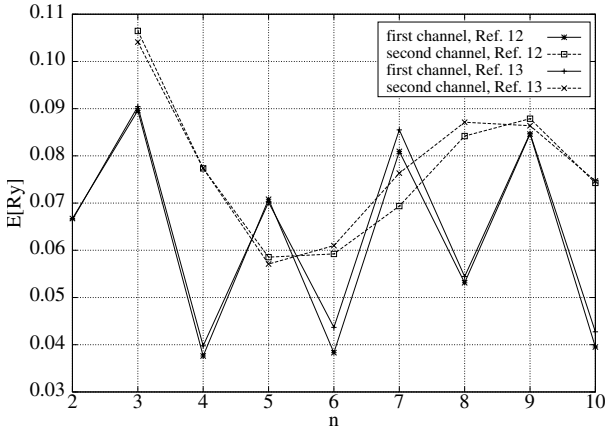

Fig. 7. Dissociation energies for Na_n^+ clusters calculated using the pseudopotentials of references [13,14] as, indicated by the markers.

the dissociation channels are in essential agreement with experimental findings of Bréchignac [21] et al.

4 Conclusion

We have described in this paper the first implementation of a fourth order operator factorization method for solving the Kohn-Sham equations with non-local pseudopotentials of the Kleinman-Bylander [2] type, which makes the application of the method for many realistic systems possible. We also have reported first results from a systematic study of Na and Mg clusters and isomers. Compared to a second order operator factorization, the fourth order method is typically an order of magnitude faster, cf. Figures 1 and 2.

This work was supported by the Spanish Ministry of Science and Education (MEC) through grant BFM2003-03372-C03 (to E.H.), the Austrian Science Fund FWF under grant No. P18134 (to E.K.) as well as the Austrian Academic Exchange Services ÖAD (11/2006) and the Spanish MEC (HU2005-0033) through a bilateral collaborative project.

References

1. W. Kohn, L.J. Sham, Phys. Rev. A **140**, 1133 (1965)
2. L. Kleinman, D.M. Bylander, Phys. Rev. Lett. **48**, 1425 (1982)
3. T.L. Beck, Rev. Mod. Phys. **72**, 1041 (2000)
4. M. Aichinger, E. Krotscheck, Comput. Mat. Sci. **34**, 188 (2005)
5. M. Suzuki, in *Computer Simulation Studies in Condensed Matter Physics*, edited by D.P. Landau, K.K. Mon, H.-B. Schüttler (Springer, Berlin, 1996), Vol. VIII, pp. 1–6
6. S.A. Chin, Phys. Lett. A **226**, 344 (1997)
7. J.P. Perdew, Y. Wang, Phys. Rev. B **45**, 13244 (1992)
8. N. Troullier, J.L. Martins, Phys. Rev. B **43**, 1993 (1991)
9. M. Fuchs, M. Scheffler, Comp. Phys. Comm. **119**, 67 (1999)
10. X. Gonze et al., Comput. Mater. Sci. **25**, 478 (2002)
11. T. Ono, K. Hirose, Phys. Rev. Lett. **82**, 5016 (1999)
12. E.R. Hernández, S. Janecek, M.S. Kaczmarski, E. Krotscheck, An evolution-operator method for Density Functional Theory, 2006, (submitted)
13. C. Fiolhas et al., Phys. Rev. B **51**, 14001 (1995)
14. S. Kümmel, M. Brack, P.-G. Reinhard, Phys. Rev. B **58**, R1774 (1998)
15. I. Moullet, J.L. Martins, F. Reuse, J. Buttet, Phys. Rev. Lett. **65**, 476 (1990)
16. I.A. Solov'yov, A. V. Solov'yov, W. Greiner, Phys. Rev. A **65**, 053203 (2002)
17. A. Lyalin, I.A. Solov'yov, A.V. Solov'yov, W. Greiner, Phys. Rev. A **67**, 063203 (2003)
18. W.A. de Heer, Rev. Mod. Phys. **65**, 611 (1993)
19. J. Akola, K. Rytkönen, M. Manninen, Eur. Phys. J. D **16**, 21 (2000)
20. F. Reuse, S.N. Khanna, V. de Coulon, J. Buttet, Phys. Rev. B **41**, 11743 (1990)
21. C. Bréchignac, P. Cahuzac, J. Leygnier, J. Weiner, J. Chem. Phys. **90**, 1492 (1989)